Supplemental Figure 1

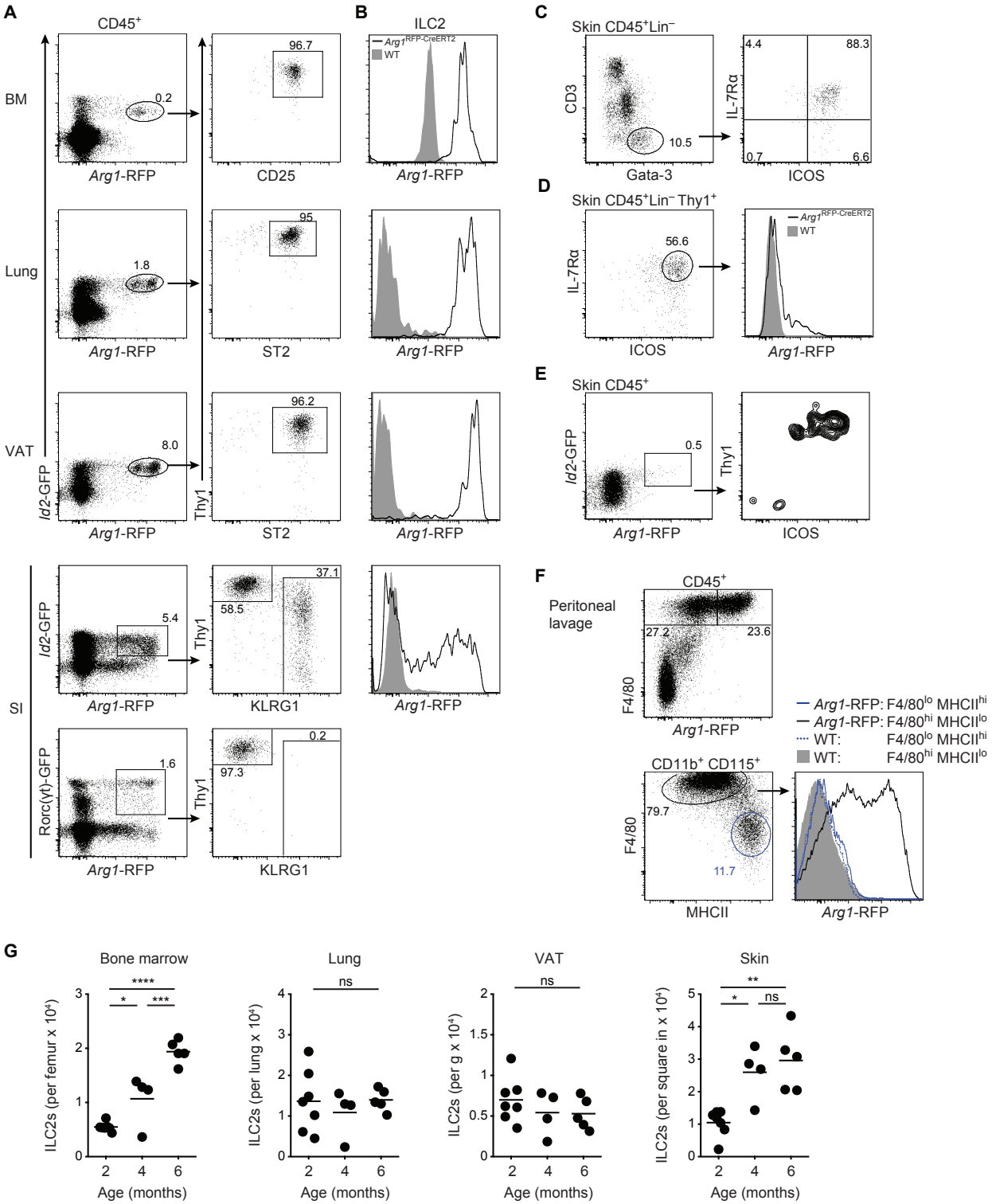

Figure S1 (related to Fig. 1). *Arg1*-RFP-CreERT2 reporter expression in ILC2s from various tissues. (A) Expression of Thy1 and CD25, ST2 or KLRG1 by *Id2*-GFP$^+$*Arg1*-RFP$^+$ or Rorc(γt)-GFP$^+$*Arg1*-RFP$^+$ cells gated on CD45$^+$ cells isolated from the indicated organs or adult *Id2*^{GFP}*Arg1*$^{RFP\text{-}CreERT2}$ or *Rorc*(γt)^{GFP}*Arg1*$^{RFP\text{-}CreERT2}$ reporter mice. (B) *Arg1*-RFP reporter expression by ILC2s of indicated organs gated as Lin$^-$Flt3$^-$IL-7Rα$^+$Thy1$^+$CD25$^+$ (BM), Lin$^-$Thy1$^+$ST2$^+$ (lung, VAT), or Lin$^-$IL-17RB$^+$KLRG1$^+$ (small intestine), isolated from WT and *Arg1*$^{RFP\text{-}CreERT2}$ mice. (C) High expression of ICOS and IL-7Rα by GATA-3$^+$ skin ILC2s. (D,E) Analysis of ILC2s in the skin of *Id2*^{GFP}*Arg1*$^{RFP\text{-}CreERT2}$ reporter mice. (D) Histograms show *Arg1*-RFP reporter expression by IL-7Rα$^+$ICOS$^+$ ILC2s pre-gated on Lin$^-$CD45$^+$Thy1$^+$ cells. (E) Expression of Thy1 and ICOS by *Id2*-GFP$^+$*Arg1*-RFP$^+$ cells gated on CD45$^+$ cells as in (A). (F) Expression of F4/80 and *Arg1*-RFP gated on CD45$^+$ cells, or of *Arg1*-RFP by F4/80^{hi}MHCI^{lo} and F4/80^{lo}MHCI^{hi} cells gated on CD11b$^+$CD115$^+$ macrophages isolated from the peritoneal cavitiy of WT and *Arg1*$^{RFP\text{-}CreERT2}$ mice. (G) Total numbers of ILC2s were determined in the indicated organs of *Arg1*$^{RFP\text{-}CreERT2}$ reporter mice at 2, 4 and 6 months of age. Data from one experiment representative of at least three independent experiments (A-F) or from one experiment (G).

Supplemental Figure 2

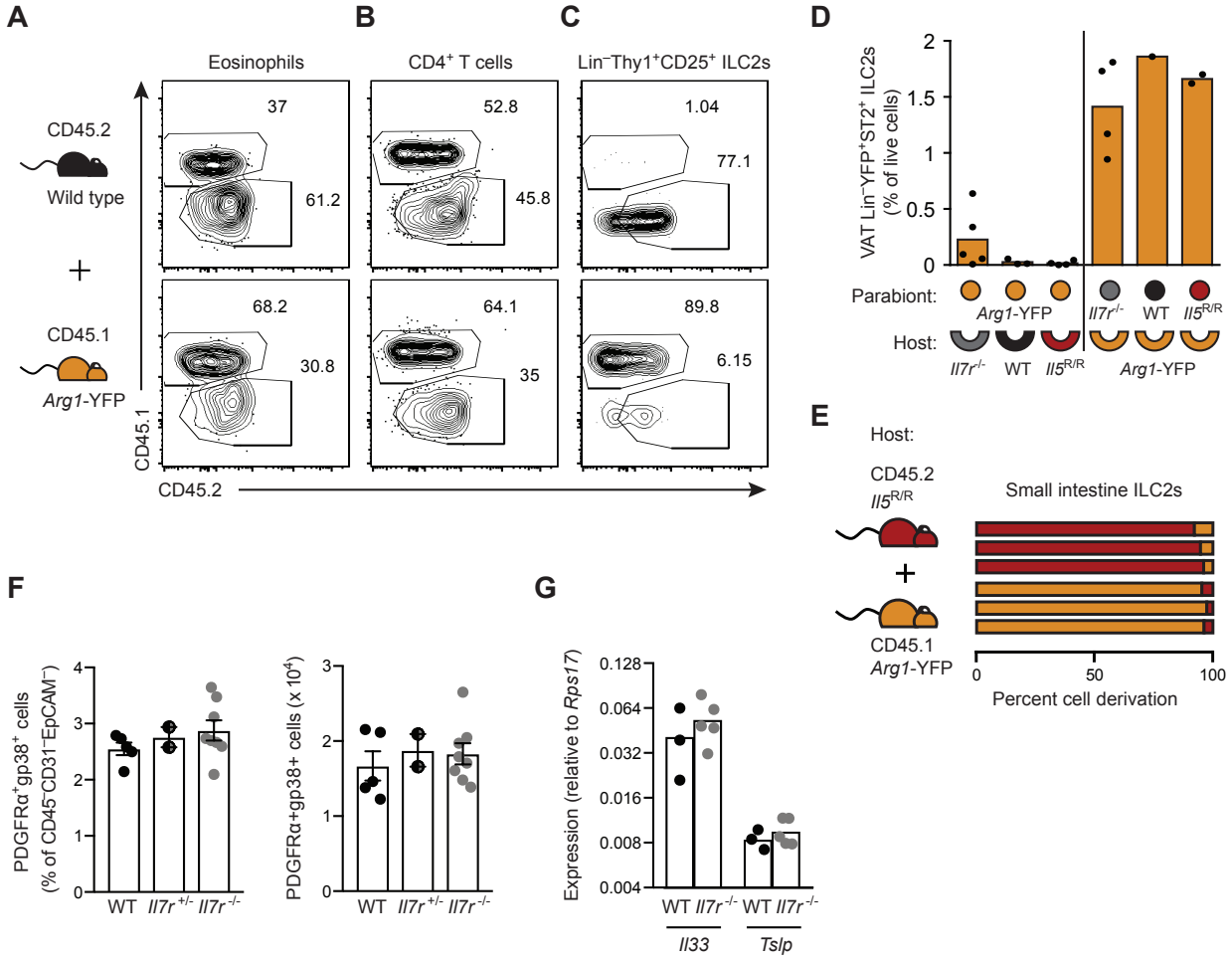

Figure S2 (related to Fig. 2). Representative flow cytometry plots and results for adipose tissue and small intestine ILC2s in parabiosis experiments. Gating to differentiate CD45.1 and CD45.2 cells among (A) eosinophils, (B) CD4+ T cells, and (C) ILC2s in the lungs of wild type CD45.2 (top) and *Arg1*-YFP CD45.1 (bottom) mice 5-6 weeks after parabiosis surgery. (D) *Arg1*-YFP^{+}CD25^{+} ILC2s in adipose tissue of host mice, enumerated as a percent of total live CD45^{+} cells, where each dot represents one host mouse, with parabionts as labeled. (E) Percent derivation of small intestine lamina propria ILC2s in *Il5*$^{R/R}$ CD45.2:*Arg1*-YFP CD45.1 pairs, where each bar represents a single mouse. (F) Percentages and numbers of CD45^{-}CD31^{-}EpCAM^{-}PDGFRα^{+}Podoplanin^{+}Sca-1^{+} stromal cells in the lung of *Il7r*$^{-/-}$, *Il7r*$^{+/-}$, and wild-type mice. (G) *Il33* and *Tslp* expression in sorted and from mice as in (F) and measured by qPCR. Data are from one surgery cohort and representative of three independent surgery cohorts (A-E), or

pooled from two independent experiments (F), or from one experiment (G). (F) Data presented as mean ± SEM.

Supplemental Figure 3

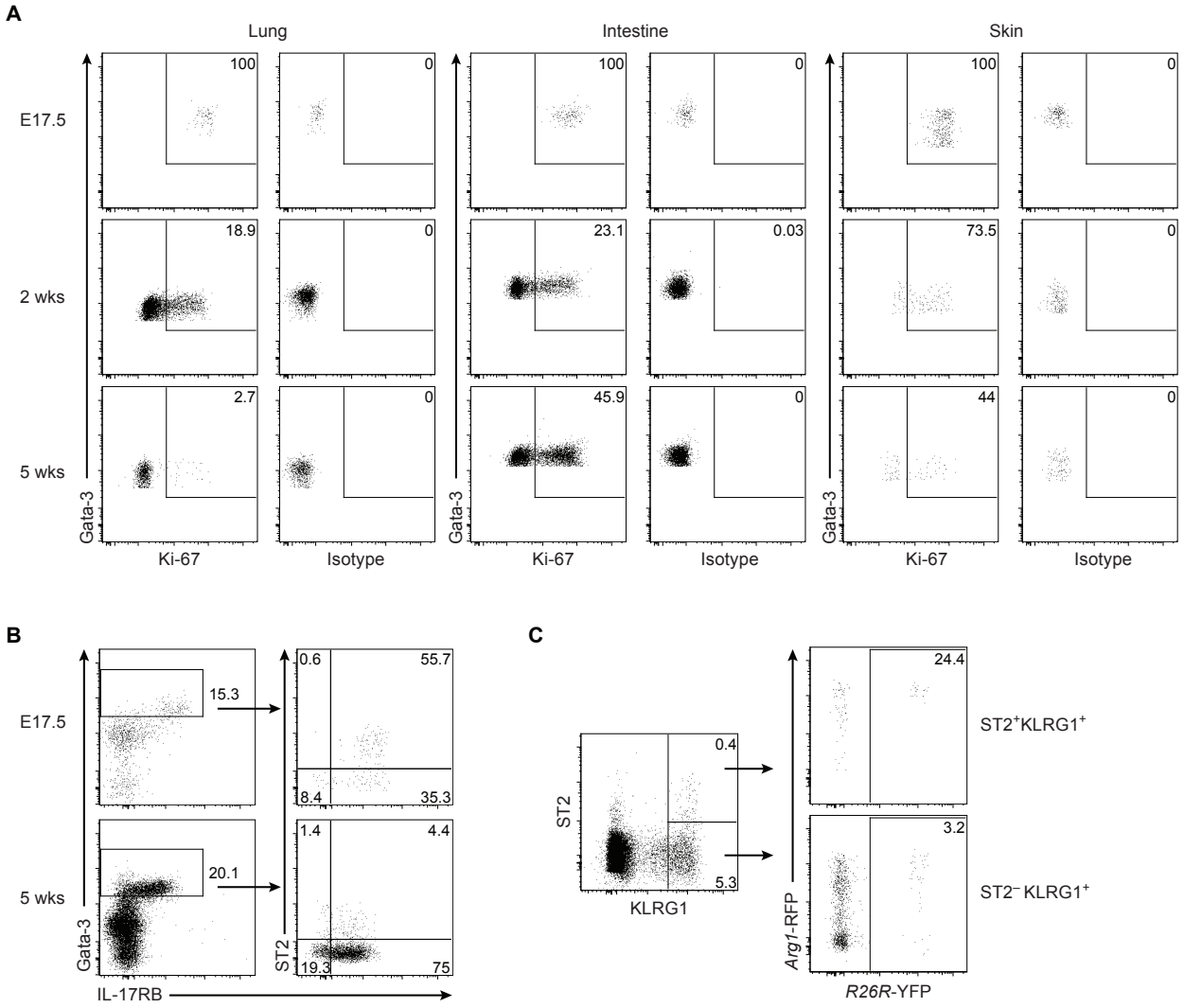

Figure S3 (related to Fig. 3). Age-dependent changes in ILC2 proliferative activity and heterogeneity in ST2 expression. (A) Intracellular staining for Ki-67 or Rat IgG2a, κ Isotype Control (eBR2a) in ILC2s gated on $Lin^{-}CD45^{+}Gata\text{-}3^{hi}$ and $ST2^{+}$ (lung), IL-$17RB^{+}$ (small intestine), or $ICOS^{+}$ (skin) cells isolated from *Arg1*$^{RFP\text{-}CreERT2}$ reporter mice at the indicated time points. (B) Expression of ST2 and IL-17RB (right) by GATA-3^{hi} cells (left) gated on Lin^{-} $CD45^{+}$ cells isolated from the lung, small intestine, and skin of mice as in (A). (C) Pregnant *Arg1*$^{RFP\text{-}CreERT2}$*R26R*^{YFP} mice were treated with tamoxifen according to the schedule in Figure 3B and the small intestine lamina propria was isolated from 2-month-old mice. Expression of *Arg1*-RFP and R26R-YFP by $KLRG1^{+}ST2^{+}$ and $KLRG1^{+}ST2^{-}$ ILC2s (pre-gated on Lin^{-} $CD45^{+}$ cells). Data from one experiment representative of at least three independent experiments.

Supplemental Figure 4

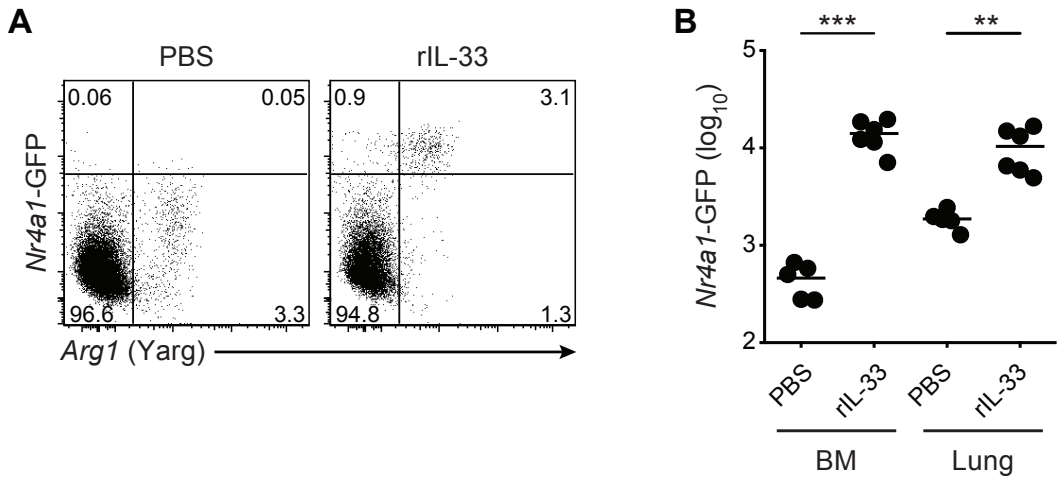

Figure S4 (related to Fig. 5). Stimulation with IL-33 results in increased Nur77 expression by ILC2s. (A,B) *Arg1*-YFP *Il5*^{Red5}*Il13*^{Sm13} *Nr4a1*-GFP reporter mice were treated with 1 μg of rIL-33 i.p. and *Nr4a1*-GFP reporter expression measured by flow cytometry in cells isolated 16h later. (A) Expression of *Arg1*-YFP and *Nr4a1*-GFP by cells gated on Lin$^-$ CD45$^+$ cells isolated from the BM. (B) The mean fluorescence intensity of *Nr4a1*-GFP in ILC2s from BM and lung of mice as in (A). Data from one experiment representative of at least two independent experiments (A) or pooled from two independent experiments (B).

Supplemental Figure 5

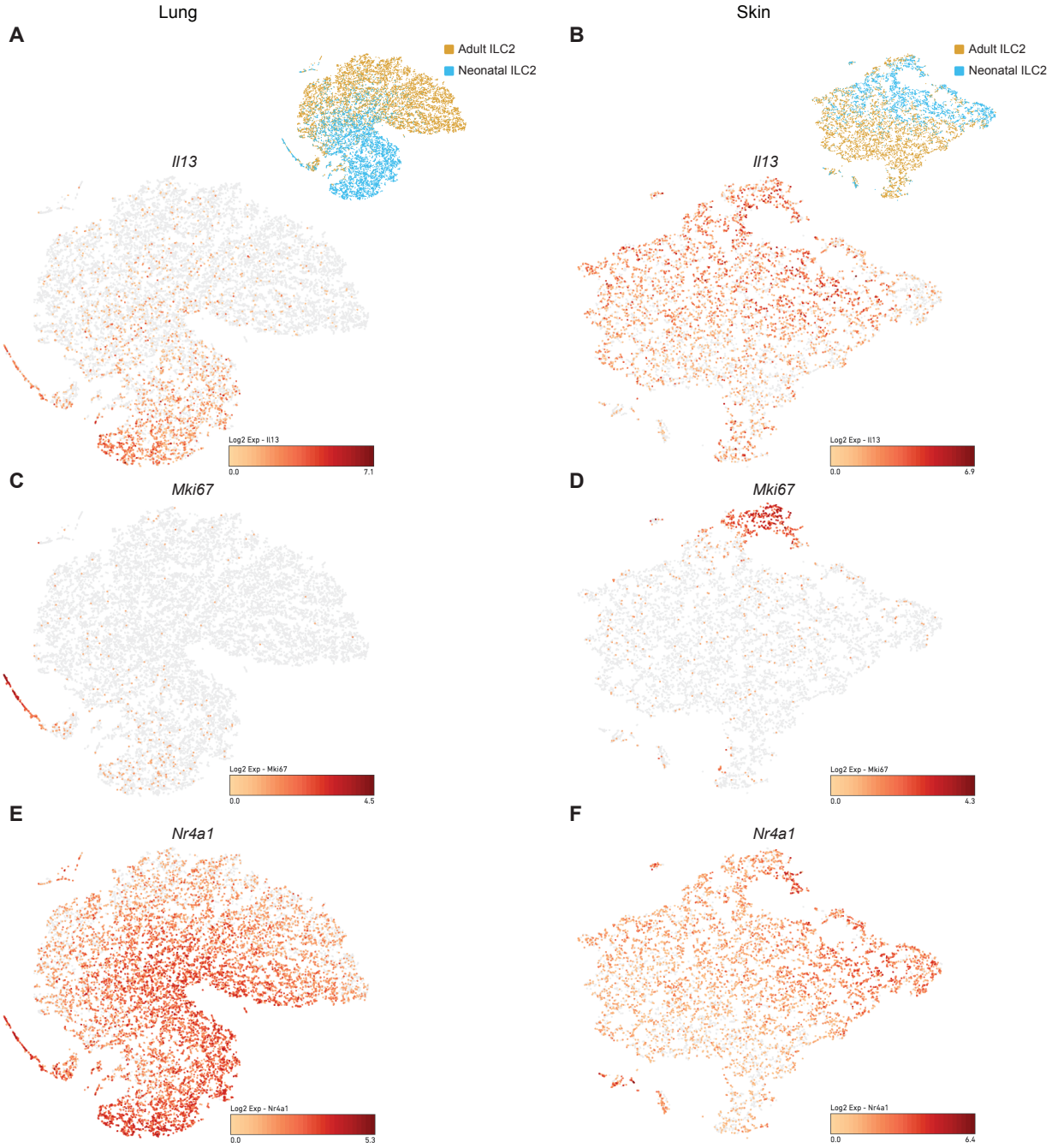

Figure S5 (related to Fig. 6). Neonatal and adult tissue ILC2 expression of *Il13*, *Mki67*, and *Nr4a1* based on single-cell RNA-sequencing analysis. (A,B) *Il13* expression visualized on t-SNE plot of single-cell RNA-sequencing data (cf. Fig. 6A,B for age of tissue of origin). (C,D) *Mki67* expression visualized on t-SNE plot of single-cell RNA-sequencing data (cf. Fig. 6A,B) (E,F) *Nr4a1* expression visualized on t-SNE plot of single-cell RNA-sequencing data (cf. Fig. 6A,B)

Supplemental Figure 6

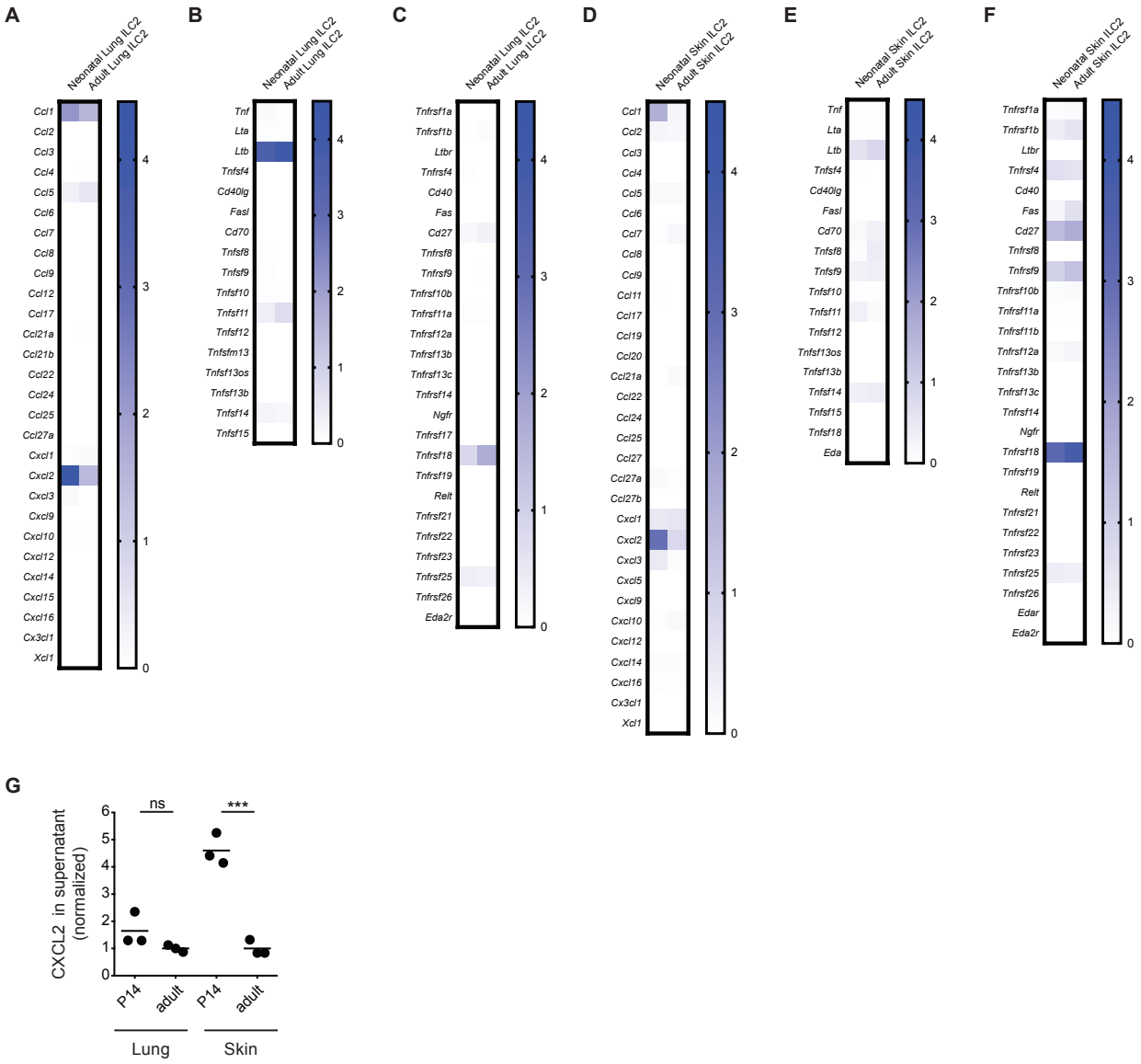

Figure S6 (related to Fig. 6). Neonatal and adult tissue ILC2 expression of chemokine genes, TNF superfamily genes, and TNFR superfamily genes. (A-F) Heatmaps showing average gene expression of chemokine, TNF superfamily, and TNF receptor superfamily genes by (A-C) neonatal and adult lung ILC2s and (D-F) neonatal and adult skin ILC2s from single-cell RNA-sequencing data analysis. (G) IL-5-reporter^{+} ILC2s were sorted from lung and skin of neonatal (p14) and adult *Il5*^{Red5} mice and cultured for 3 days with rIL-2, rIL-7 and rIL-33. The concentration of CXCL2 in the supernatant was analyzed by ELISA

and normalized to the concentration form adults. Data is from one experiment and data points represent wells with ILC2s sorted from individual mice.